How to Cite: Balyasin, M.V., Serpionov, G.V., Krasheninnikov, M.E., Lyundup, A.V., & Nechaev, A. N. (2025). Biological Compatibility of Polyethylene Terephthalate Track Membranes: Growth, Proliferation, and Viability of Cells in Culture Systems. *Eurasian Journal of Chemistry, 30, 3(119), 99-109.* https://doi.org/10.31489/2959-0663/3-25-5

Article

Received: 26 May 2025 | Revised: 15 August 2025 |
Accepted: 27 August 2025 | Published online: 21 September 2025

UDC 577.35+ 620.1

https://doi.org/10.31489/2959-0663/3-25-5

Maksim V. Balyasin[1], Genrikh V. Serpionov[2*], Mikhail E. Krasheninnikov[1], Alexey V. Lyundup[1], Alexander N. Nechaev[2]

[1]Peoples' Friendship University of Russia named after Patrice Lumumba, Moscow, Russia;
[2]Joint Institute for Nuclear Research, Dubna, Moscow region, Russia
*(*Corresponding author-mail: genrihserpionov@gmail.com)*

Biological Compatibility of Polyethylene Terephthalate Track Membranes: Growth, Proliferation, and Viability of Cells in Culture Systems

This study evaluated the biocompatibility of polyethylene terephthalate track membranes (PET TMs) obtained by heavy ion irradiation followed by chemical etching, with respect to cell growth, proliferation, and viability in culture systems. Physical parameters of the PET TMs were determined, including Young's modulus, ultimate tensile strength, and contact angle. Cytotoxicity of PET TMs was studied on three cell cultures: the epithelial line MCF7 (adenocarcinoma), fibroblast-like mouse line 3T3, and a primary culture of mesenchymal stromal cells (MSCs) isolated from rabbit bone marrow. Cytotoxicity was assessed using two methods: extraction from the material and the direct contact method in accordance with the Interstate Standard ISO 10993-5-2011, IDT. The results demonstrated that neither PET TM extracts nor direct contact samples significantly affected cell growth. The proliferation rate of MCF7 cells was 0.01531 1/h for the extract and 0.01568 1/h for direct contact, which did not differ statistically from the control group (0.01877 1/h, $p = 0.138$). Microscopic analysis confirmed the preservation of cellular morphology: MCF7 cells retained cuboidal morphology, while 3T3 cells exhibited a spindle-shaped morphology. Real-time cell analysis (RTCA) revealed no significant effect of the tested samples on the cellular index (C_i), further supporting the absence of a cytotoxic effect. Visual observations of cell cultures after incubation with the studied samples also did not reveal cell confluence and morphology changes. These findings provide important evidence for the safety of PET TMs in biomedical research and cell culture systems, recommending them for further research in tissue engineering and regenerative medicine.

Keywords: heavy ion irradiation, chemical etching, track-etched membrane, polyethylene terephthalate, regenerative medicine, cytotoxicity, cell culturing, tissue engineering

Introduction

Track membranes (TMs) are thin polymer films (5–30 μm in thickness) with a pore system of strictly defined geometry. They are obtained by irradiating the polymer film with heavy ions followed by chemical etching to form nano- and micropores [1]. The most widely used TMs are made of polyethylene terephthalate (PET) and polycarbonate (PC). TMs have broad applications in medicine and biochemistry [2], including biological and chemical sensing [3–5], water purification [6, 7], electrophoresis [8], plasmapheresis [9], and numerous other technological and biomedical processes. In addition, TMs are employed in cell cultivation systems, particularly in Transwell systems [10–12]. Transwell systems (TS) are containers for cell cultivation that enable the creation of bi- or multilayer cellular models [13] with static or dynamic movement of the culture medium. They typically consist of two chambers: an apical chamber with a semipermeable membrane installed at the bottom and a basolateral chamber. These systems are widely used for two-dimensional (2D) and three-dimensional (3D) cell cultivation. In 2D culturing, membranes provide a flat surface that allows studying cell adhesion, proliferation, and morphology. In the case of 3D culturing, TMs support multilayer co-cultivation of different cell types, with distinct cell populations adhering to each side of the membrane as well as to the bottom of the basolateral chamber. This setup mimics tissue–tissue interactions *in vivo*, which is particularly important for tissue engineering and regenerative medicine, studies of pathological processes such as carcinogenesis, investigations of specific cell functions, and the analysis of tissue barrier properties [13–16].

Numerous studies have utilized TS to develop *in vitro* models of the intestinal epithelial barrier, enabling the investigation of absorption [17], interactions with pathogenic microorganisms [18], drug screening [19], and evaluation of drug-induced toxicity [20]. TS have also been applied to generate artificial blood-

brain barrier models for studying immune cell migration into the CNS, a key feature of multiple sclerosis pathogenesis [21, 22]. Furthermore, these systems have been used to investigate the function of brain endothelial cells by co-cultivating endothelial cells with astrocytes or pericytes [23, 24].

Transwell analysis is traditionally used to assess the migratory and invasive activity of tumor cells. Li et al. (2018) used TS for tumor cells' migratory study. It was demonstrated that depletion of the active pool of Prdx1 protein reduced the invasive and migratory capacity of colorectal cancer cells, whereas increased Prdx1 expression produced the opposite effect [25]. Using TS, Zhao et al. (2022) showed that miR-29b-3p microRNA exerted an inhibitory effect on the proliferation, invasion, and migration of 22Rv1 prostate cancer cells [26]. TS have also been applied to investigate the impact of ICOS gene expression on the invasive potential of hepatocellular carcinoma cells [27]. The inhibitory role of secretory cGMP-dependent protein kinase type II (PKG II) in the migration, invasion, and proliferation of gastric cancer cells was likewise demonstrated using TS [28]. Furthermore, Jeon et al. (2016) employed TS to study the influence of mitochondria on invasion and migration in drug-resistant lung adenocarcinoma cells [29].

TS have been applied to study amyloidogenesis, prion transfer between cells, and the processes of amyloid absorption by macrophages in the presence of various amyloid neurodegenerative diseases [30–33]. In addition, TM-based systems have been used to investigate the effect of the spatial organization of the cell culture of fibroblast-like cells and dermal fibroblasts on the level of expression of bone remodeling markers [34] and the level of fibroblast migration [35].

Track-etched membranes have also been employed in the development of "organ-on-a-chip" systems. Organs on chips (organ chips) are microfluidic cell culturing devices containing continuously perfused hollow microchannels populated with living cells. This design enables simulation of physiological processes at the tissue and organ levels, offering a potential alternative to animal experiments in the future [36]. Furthermore, track membranes are integral components of multi-chamber microfluidic devices [37, 38].

The quantitative method of transepithelial/transendothelial electrical resistance (TEER) is widely used for measuring the integrity of tight junction dynamics in cell culture models of endothelial and epithelial monolayers. TEER values serve as reliable indicators of the integrity of cellular barriers prior to evaluating the transport of drugs or chemicals. TEER measurements can be performed in real time without damaging the cells. A classic TEER setup consists of a cell monolayer cultured on a semipermeable filter insert, which separates the system into apical (upper) and basolateral (lower) compartments. For electrical measurements, two electrodes are used: one placed in the upper compartment and the other in the lower one, separated by a cell monolayer. In these devices, TMs serves as substrates for cell growth, forming a monolayer through which electrical resistance is measured. They provide a controlled porous structure that promotes cell adhesion, growth, and differentiation [38, 39].

Despite the widespread use of TS for culturing various cell lines and microfluidic devices equipped with TMs, there is limited information in the literature regarding the influence of TM chemical composition on cell growth and proliferation, as well as on their potential cytotoxicity.

Several studies have examined the toxicity of bisphenol A, a monomer unit of polycarbonate membranes, and the degree of its extraction from the polymer [40–44]. These findings are relevant for evaluating the toxicity of polycarbonate films, as they undergo alkaline hydrolysis and are exposed to aqueous environments during cell cultivation. In contrast, no studies have directly assessed the cytotoxicity of PET TMs. Nevertheless, some reports indicate that PET, in the form of nano- and microgranules, can exhibit toxic effects [45, 46].

Therefore, the present study aims to investigate the impact of the chemical composition of PET TMs on cell growth, proliferation, and viability, with a particular focus on evaluating potential cytotoxicity. The results obtained in this study may be utilized to assess the feasibility of applying PET TMs in regenerative medicine, particularly as a component of implantable biological capsules carrying living cells.

Experimental

Preparation of TMs for Working with Cell Cultures

To fabricate TMs with cylindrical pores, a high-quality polyester polyethylene terephthalate film was used ("PJSC Chemical Plant, Vladimir, Russia, premium grade, State standard No. 24234-80) with a thickness of 11 μm. The film was irradiated with accelerated heavy ions using an IC 100 cyclotron. The irradiated samples were then subjected to ultraviolet (UV) sensitization followed by chemical etching. Detailed production conditions and membrane characteristics are described by Apel et al. (2021) [47]. Final-

ly, the resulting membranes were sterilized by autoclaving at a temperature of 121 °C and a pressure of 1 atm for 60 minutes.

Measurement of the mechanical characteristics of TMs

The tensile mechanical properties of the investigated films were measured at room temperature using a Shimadzu AGS-X testing machine equipped with a 50 N load cell. Rectangular samples with a width of 10 mm and a gauge length of 35 mm were stretched at a rate of 1 mm/min. The sample thickness was measured by a Mitutoyo litematic vl-50 thickness tester (measuring force 0.01 N). The stress and strain parameters were calculated using the Trapezium X software.

Hydrophilic-Hydrophobic Properties of TMs

The degree of hydrophilicity of the polyester films and TMs was determined by measuring the contact angle of wetting with water (θ°) using the "sitting drop" method on a DSA-100 device (KRÜSS, Germany).

Scanning Electron Microscopy (SEM)

A high-resolution scanning electron microscope, FESEM SU-8020 (Hitachi, Tokyo, Japan), was used for morphological analysis of the surface, as well as the number and diameter of pores in PET TMs. The examination was conducted in the secondary electron (SE) registration mode at an accelerating voltage of 3 kV with a magnification of 5×10^4 times. Prior to examination, a 15 nm layer of platinum-palladium alloy was deposited onto the samples by magnetron sputtering using a Quorum Q150T S system.

Cell Cultures

The cell cultures were provided by the leading researcher M.E. Krasheninnikov (Research and Educational Center "Cell Technologies", Peoples' Friendship University of Russia named after Patrice Lumumba, Moscow, Russia). Linear cell cultures and primary cell culture were selected for the work: MCF7 — a line of human epithelial cells (adenocarcinoma); 3T3 — a line of mouse embryonic immortalized fibroblasts; MSC — mesenchymal stromal cells isolated from rabbit bone marrow. Multipotent cells with the ability to differentiate in the adipo-, osteo- and chondrogenic direction, as well as the ability to actively proliferate. They have a fibroblast-like, spindle-shaped morphology. All cells were tested for the absence of mycoplasma contamination prior to experiments using a chemiluminescent detection system (Servicebio, China). Rabbit MSCs were maintained in T75 culture flasks (Sarstedt, Germany) in DMEM/F12 medium (Himedia, India) supplemented with L-glutamine, 10 % FBS (Himedia, India), insulin 1.6 μg/ml (PanEco, Russia), FGF2 — 4 ng/ml (FGF2, Israel), dexamethasone 2 nM (Russia), penicillin-streptomycin (PanEco, Russia), passaged every 3 days 1/5 no more than 5 passages, under conditions of +37 °C, high humidity and an atmosphere of 5 % CO_2.

MCF7 and 3T3 cell cultures were maintained in T75 culture flasks (Sarstedt, Germany) in DMEM/F12 culture medium (Himedia, India) supplemented with L-glutamine, 10 % FBS (Himedia, India), and penicillin-streptomycin (PanEco, Russia), passaged every 3 days 1/10, under conditions of +37 °C, high humidity and 5 % CO_2 atmosphere.

Cytotoxicity

Cytotoxicity testing was performed in accordance with the Interstate Standard ISO 10993-5-2011, "medical devices. evaluation of the biological effect of medical devices". Part 5. Cytotoxicity studies: *in vitro* methods" [48]. In accordance with the Interstate Standard, the studies were performed on: 1) an extract from the material; 2) on the material itself (direct contact method). Phosphate buffered saline (PBS) with normal pH (7.2) and physiological osmolarity was selected as the eluent. In the control group, a 1:1 mixture of PBS and culture medium was applied. In the extract group, the extract was added in a 1:1 PBS solution with the culture medium. In the direct contact group, PET TMs were placed directly into the culture, with a 1:1 PBS-to-culture medium mixture added. Two methods, described below, were employed to assess cytotoxicity.

Extract Preparation

Extracts were prepared under conditions of 121 °C and 1 atm for 1 hour. PET TM samples at 1.6 ± 0.2 mg/cm^2 were immersed in sterile phosphate-buffered saline (PBS, pH 7.2; PanEco, Russia). The final material-to-solution ratio was 1.6 ± 0.2 mg/ml.

Preparation of Test Samples

Metal punches with a diameter of 10 mm and an area of 0.79 cm^2 were used to prepare PET TM samples for direct contact. The material was cut on a silicone substrate and subsequently sterilized in PBS under the specified conditions in a volume of 1 cm^2 per 1 ml of solution.

Cytotoxicity (Imaging)

Imaging was chosen as the primary method for assessing cytotoxicity, using automated inverted microscopy with photo and video recording under continuous culture conditions (37 °C, 5 % CO_2, and high humidity). MCF7 and 3T3 cell cultures were seeded into 24-well plates (10,000 cells/cm^2; well surface area = 2 cm^2) according to Table 1. After 24 h, the test samples were introduced, and cultivation was continued for an additional 3 days. The criterion for cytotoxicity was a significant difference in confluency (a characteristic of the area occupied by the cell culture during cultivation) at the end of the experiment (a difference of more than 20 % confluency) for samples with a weak cytotoxic effect or a visible change in morphology for samples with a pronounced cytotoxic effect (growth arrest, cell death, balling and detachment).

Real-Time Cellular Cytotoxicity Assay (RTCA)

The real-time cellular assay (RTCA) is a non-invasive method based on continuous measurement of cellular impedance. This approach employs gold microelectrodes embedded in the bottom of a microtiter plate well to monitor resistance to electron flow in a conductive solution. When adherent cells attach to the electrodes, they impede the flow of current, which is quantified by the dimensionless parameter Cell Index (C_i), where C_i = (resistance at time n — resistance in the absence of cells) / nominal resistance value. An increase in C_i over time reflects cell proliferation, eventually plateauing at 100 % confluence. Introducing an apoptosis inducer or cytotoxic substance decreases C_i to zero, reflecting the detachment of cells from the well bottom. Thus, the RTCA method provides quantitative data on cell number, their proliferation, size/shape, and quality of attachment to the substrate; C_i is a cell index based on the measurement of cellular impedance during cell culture growth, the change in which is interrelated with proliferation, CPE, cytostatic effect or cytotoxicity.

RTCA was chosen as an additional method for determining cytotoxicity. For this purpose, cMSCs were seeded at a density of 10,000 cells/cm^2 (well area 0.32 cm^2) into 16-well E-plates equipped with gold electrodes to measure the cellular index (C_i). After that, the onset of the active growth phase was expected, and materials were added in accordance with Table 2. Cultivation was carried out until a plateau was reached. For the negative control, a 0.2 % SDS solution 1:1 to the culture medium was added to the control well after reaching the plateau. To normalize the effect of the extract or PET TM on C_i, background subtraction was performed during post-processing of the data, with negative values set to zero.

The criterion for cytotoxicity was a statistically significant difference in the k coefficient (C_i, 1/h) for samples with a weak cytotoxic effect, or a low C_i value after reaching a plateau (<50 % of the maximum) as a result of adding the test substance, for samples with a pronounced cytotoxic effect.

Statistical Analysis

Data processing was performed in Excel (Microsoft, USA). Statistical analysis was performed in GraphPad Prism version 9.5.1 (USA). To compare the growth rate between groups, a mathematical model of exponential growth with a plateau was applied

$$y = y_m - \left(y_m - y_0\right) \times e^{-k \times x},$$

where y_m is the maximum C_i, y_0 is the initial C_i, and k is the growth rate of C_i 1/h.

The acceptability of the calculated models was assessed using the R^2 coefficient. Differences in growth rate (k, 1/h) between the study groups were assessed using the F criterion. The data on the graph are given as the mean ± standard deviation (SD). Statistical significance was accepted at p <0.05.

Results and Discussion

Characteristics of TM Surface Morphology

Porosity and pore diameter were determined from scanning electron microscopy (SEM) micrographs (Fig. 1). The characteristics of TMs are presented in Table 3.

Physical Properties of TMs

In this study, the hydrophobic-hydrophilic and mechanical properties of PET TMs were investigated (Table 4). In addition, based on a comprehensive literature review, values for the zeta potential and surface charge of these membranes are presented. The isoelectric point (pI) of PET TMs generally lies between 3.5 and 4 [49], indicating that under physiological conditions (pH = 7.0), they carry a net negative charge. This is consistent with the findings of Sabbatovskii et al. (2012), who reported that PET TMs with a pore diameter of 25 nm exhibit a zeta potential of approximately −27 mV (pore density ~2 × 10^9 pores/cm^2, measured in 0.25 M KCl solution). Furthermore, the same study demonstrated that membranes with pore diameters ranging from 13 to 80 nm consistently possess a negative surface charge, with surface charge density (σ) values on the order of (1–100) × 10^4 C/m^2 under varying electrolyte concentrations [50]. The observed negative values of zeta potential and surface charge have been attributed to the presence of carboxyl functional groups on the membrane surface [51]. Importantly, the magnitude of the surface zeta potential, and thus the surface charge density of PET TMs, can be strongly influenced by parameters such as membrane pore size, the pH of the surrounding medium, and ionic strength of the solution [52, 53]. Taken together, the negative zeta potential and associated surface charge characteristics facilitate favorable electrostatic interactions between PET TM surfaces and cellular membranes, thereby promoting enhanced cell adhesion on the PET TM substrate [54, 55].

The contact angle was found to range from 67° to 75°, indicating that PET TMs possess moderately hydrophilic properties. This degree of wettability is considered optimal for efficient cell adhesion to the polymer surface, as demonstrated for mouse fibroblast cell lines [56] and HUVEC cells [57]. Such wettability provides a balance between adhesive and repulsive interfacial forces, thereby enhancing cellular attachment. Moreover, a surface contact angle of approximately 70° was reported to promote increased migration of HUVECs [57]. Similarly, Margel et al. (1993) demonstrated using canine endothelial cells that contact angle values within this range correspond to high levels of adhesion and proliferative activity [58].

Substrates with varying mechanical properties are used for culturing different cell lines [59]. In this study, the Young's modulus of the PET TMs was determined to be 2871 ± 157 MPa. Materials with stiffness comparable to that of TM (~3 GPa) used in the present study have been previously employed to investigate the behavior of vascular smooth muscle cells, endothelial cells, and chondrogenic cells, demonstrating the relevance of high-stiffness substrates in modulating cellular responses [60–62].

Therefore, PET TMs physical properties enable its effective application in cell biology research and tissue engineering by providing optimal conditions for cell adhesion, migration, and proliferation.

Sterilization of PET TM

After autoclaving at 121 °C for 1 h, PET TMs showed no visible changes in shape, remained intact, and retained their transparency. These observations confirm the suitability of this sterilization method for subsequent sample preparation.

Cytotoxicity

Culturing MCF7 and 3T3 cells with the extracts of the tested samples, as well as under direct contact conditions, revealed no effect on the growth rate of the cell cultures (Fig. 2 *a*, *b*). MCF7 cells exposed to both extract and direct contact retained their cuboidal, epithelial-like morphology. The samples did not affect cell proliferation, and no differences in confluence were observed at the end of the experiment. Thus, no cytotoxic effect on MCF7 cells was detected. Similarly, 3T3 cells maintained their elongated, fibroblast-like morphology under both conditions. The samples did not affect proliferation, and no cytotoxic effect on 3T3 cells was detected.

The RTCA method and measurement of the cellular index C_i on the culture of cMSC cells also showed no significant effect on the rate of cell proliferation (Table 5, Fig. 3 *a*, *b*). For comparison, to induce a pronounced cytotoxic response, sodium dodecyl sulfate (SDS) was added to the control group 164 h after the start of cultivation. This treatment, which disrupts cell membranes, causes detachment from the culture surface, and releases cellular proteins, DNA, lipids, and other components into the medium, led to a sharp decline in C_i.

It was noted that the studied samples slightly reduced the maximum value of the cellular index C_i. The growth rate of C_i in the groups (coefficient k) of extract, direct contact, and control was 0.01531, 0.01568, and 0.01877 per hour, respectively. There was no statistically significant difference in the coefficient k between the groups (p value = 0.138).

Table 1

Scheme for adding samples and cell cultures to a 24-well plate

	1	2	3	4	5	6
A	–	–	MCF7, Extract 1:1	MCF7, Direct contact	3T3, Extract 1:1	3T3, Direct contact
B	–	–	MCF7, Extract 1:1	MCF7, Direct contact	3T3, Extract 1:1	3T3, Direct contact
C	–	–	MCF7, Extract 1:1	MCF7, Direct contact	3T3, Extract 1:1	3T3, Direct contact
D	–	–	MCF7, Control	MCF7, Control	3T3, Control	3T3, Control

Table 2

Scheme of adding samples and cell cultures to a 16-well e-plate

No.	1	2
A	MSC, Extract 1:1	MSC, Extract 1:1
B	MSC, Extract 1:1	MSC, Extract 1:1
C	MSC, Extract 1:1	MSC, Direct contact
D	MSC, Direct contact	MSC, Direct contact
E	MSC, Direct contact	MSC, Direct contact
F	MSC, Control	MSC, Control
G	MSC, Control	Direct contact
H	Extract 1:1	PBS

Table 3

Characteristics of TM obtained by SEM

PET TM	Thickness, μm	Pore density, cm^{-2}	Pore diameter, nm	Porosity, %
	10.8±0.3	$(8±0.7) \times 10^9$	25±5	3.68±0,21

Table 4

Physical properties of PET TM

Parameter	Young's modulus, *E* (MPa)	Ultimate strength, σ_B (MPa)	Contact angle, θ° (side A/ side B)
Value	2871±157	71±5	67.31±1.97 / 75.02±1.40

Table 5

Results of mathematical modeling of rabbit MSC cell culture growth (C_i)

Parameters	Extract 1:1	Direct contact	Control	*p* value, (F [DFn, DFd])
k (1/h)	0.015±0,003	0.016±0,002	0.019±0,002	0.138 (1.986 [2, 693])
R^2	0.89	0.96	0.97	

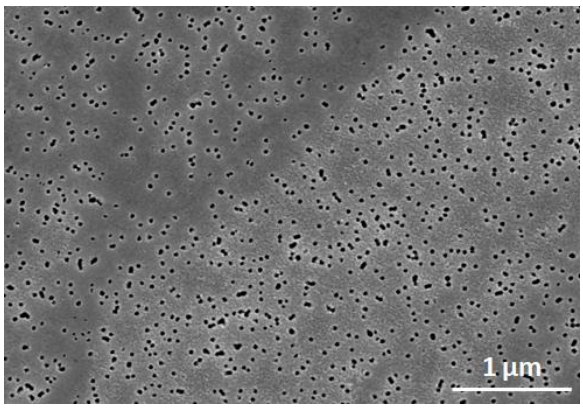

Figure 1. SEM micrographs of the PET TM surface

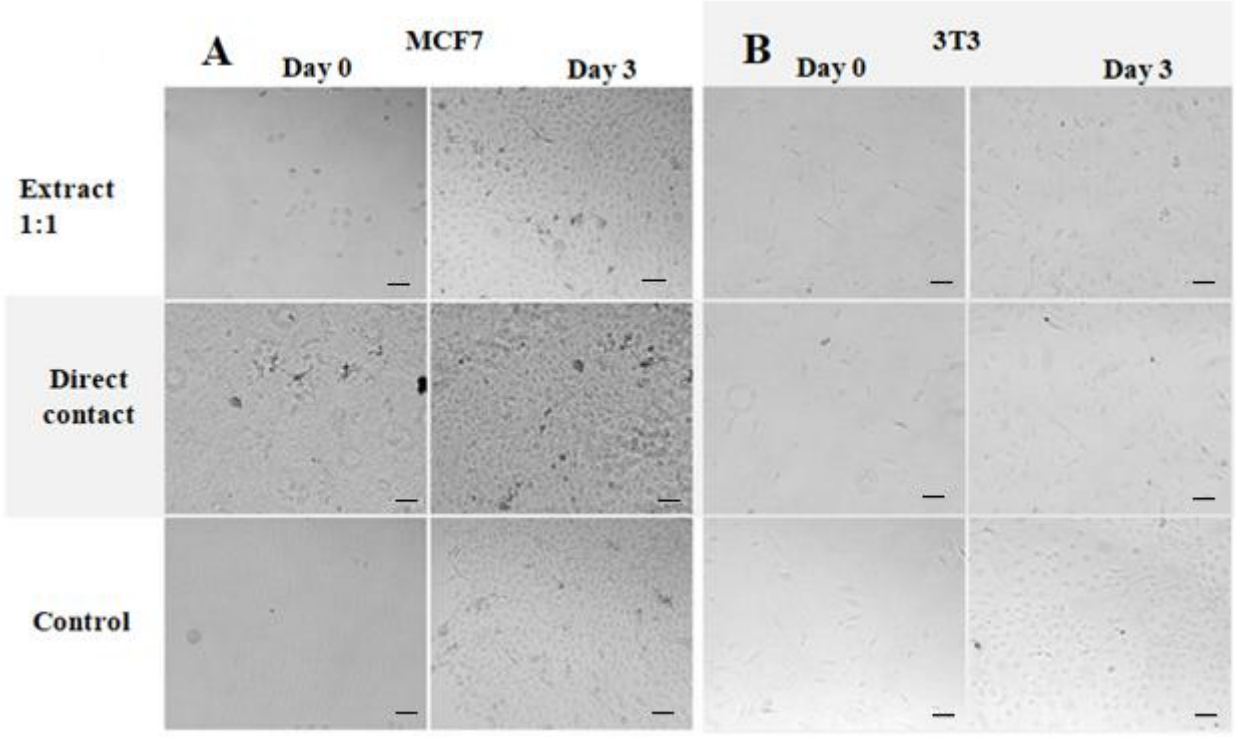

Figure 2. (*a*) — Effect of the extract and direct contact on the growth of the MCF7 cell culture compared to the control group during interaction with the test substance for 5 days; (*b*) — Effect of the extract and direct contact on the growth of the 3T3 cell culture compared to the control group during interaction with the test substance for 5 days; Objective 10× (Ph), timelapse 78 hours, shooting interval 40 minutes. Scale bar: 50 µm

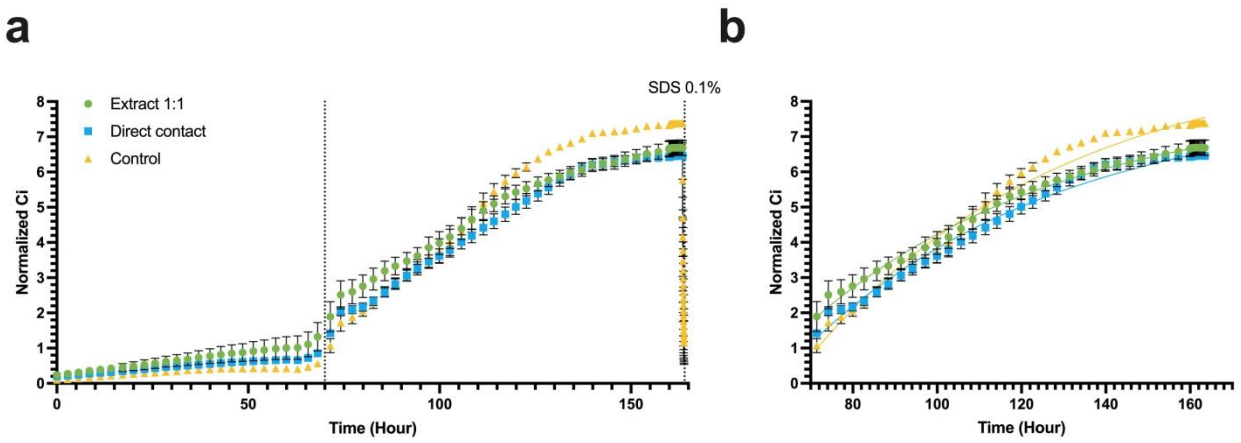

Figure 3. (*a*) — A growth rate of rabbit MSC cell culture, the dependence of C_i on time; (*b*) — interval 70–164 hours selected for subsequent statistical analysis, point 70 hours is taken as 0; data are presented as mean ± SD

Conclusions

The cytotoxicity of PET TM was assessed using two methods on three cell cultures (the epithelial line MCF7, the 3T3 fibroblast-like line, and primary rabbit MSC BM culture) in accordance with the Interstate standard ISO 10993-5-2011, IDT, medical devices. Evaluation of the biological effect of medical devices, Part 5, cytotoxicity studies: *in vitro* methods. The results demonstrated that PET TM samples did not affect cell cultures, the proliferation rate and cell morphology. The cytotoxicity assessment confirmed that PET TM samples are non-cytotoxic. Based on these findings, PET TMs can be recommended for further biomedical research, including their application in tissue-engineered constructs and for the encapsulation of cellular preparations intended for long-term therapeutic use.

Funding

This research was funded by JINR Project No. 07-5-131-2-2024/2028.

*Author Information**

*The authors' names are presented in the following order: First Name, Middle Name and Last Name

Maksim Vitalievich Balyasin — Junior Researcher, Peoples' Friendship University of Russia named after Patrice Lumumba, Miklukho-Maklaya Street, 6, 117198, Moscow, Russia; e-mail: b.maxim4432@yandex.ru; https://orcid.org/0000-0002-3097-344X

Genrikh Vladimirovich Serpionov (*corresponding author*) — Candidate of Biological Sciences, Researcher, Joint Institute for Nuclear Research (JINR), Joliot-Curie Street, 6, Dubna, Moscow Region, 141980, Russia; e-mail: genrihserpionov@gmail.com; https://orcid.org/0009-0001-4545-8811

Mikhail Evgenievich Krasheninnikov — Candidate of Biological Sciences, Leading Researcher, Peoples' Friendship University of Russia named after Patrice Lumumba, Miklukho-Maklaya Street, 6, 117198, Moscow, Russia; e-mail: krashen@rambler.ru; https://orcid.org/0000-0002-3574-4013

Alexey Valerievich Lyundup — Candidate of Medical Sciences, Director of the Research and Educational Center "Cell Technologies", Peoples' Friendship University of Russia named after Patrice Lumumba, Miklukho-Maklaya Street, 6, Moscow, 117198, Russia; e-mail: lyundup2020@gmail.com; https://orcid.org/0000-0002-0102-5491

Alexander Nikolaevich Nechaev — Candidate of Chemical Sciences, Deputy Director for Science, Centre of Applied Physics, Joint Institute for Nuclear Research (JINR), Joliot-Curie Street, 6, 141980, Dubna, Moscow Region, Russia; e-mail: nechaeffalexander@yandex.ru; https://orcid.org/0000-0002-5138-4265

Author Contributions

The manuscript was prepared with contributions from all authors, and all authors have approved the final version for submission. CRediT: **Maksim Vitalievich Balyasin** data curation, investigation, conducting biological experiments, methodology, validation, visualization, writing-review & editing; **Genrikh Vladimirovich Serpionov** data curation, investigation, characterization of physical properties of TMs, methodology, validation, visualization, writing-review & editing; **Mikhail Evgenievich Krasheninnikov** investigation, methodology, validation, formal analysis, supervision, validation, writing-review & editing; **Alexey Valerievich Lyundup, Alexander Nikolaevich Nechaev** conceptualization, writing-review & editing, funding acquisition, resources, supervision, validation, writing-review & editing.

Acknowledgments

The authors sincerely thank Pavel Apel for his valuable and precise feedback during the manuscript preparation, Oleg Orelovich for supplying the electron micrographs, and Maria Kuvaytseva for her assistance with the contact angle measurements.

Conflicts of Interest

The authors declare no conflict of interest.

References

1 Apel, P. (2001). Track etching technique in membrane technology. *Radiation Measurements, 34*(5), 559–566. https://doi.org/10.1016/S1350-4487(01)00228-1

2 Dolfus, C., Piton, N., Toure, E., & Sabourin, J. C. (2015). Circulating tumor cell isolation: The assets of filtration methods with polycarbonate track-etched filters. *Chinese Journal of Cancer Research, 27*(5), 479–487. https://doi.org/10.3978/j.issn.1000-9604.2015.09.01

3 Kaya, D., & Keçeci, K. (2020). Review—Track-Etched Nanoporous Polymer Membranes as Sensors: A Review. *Journal of The Electrochemical Society, 167*(3), 037543. https://doi.org/10.1149/1945-7111/ab67a7

4 Mizuguchi, H., Sasaki, K., Ichinose, H., Seino, S., Sakurai, J., Iiyama, M., Kijima, T., Tachibana, K., Nishina, T., Takayanagi, T., & Shida, J. (2017). A triple-electrode based dual-biosensor system utilizing track-etched microporous membrane elec-

trodes for the simultaneous determination of l-lactate and d-glucose. *Bulletin of the Chemical Society of Japan, 90*(11), 1211–1216. https://doi.org/10.1246/bcsj.20170193

5 Torati, S. R., Reddy, V., Yoon, S. S., & Kim, C. (2016). Electrochemical biosensor for Mycobacterium tuberculosis DNA detection based on gold nanotubes array electrode platform. *Biosensors and Bioelectronics, 78*, 483–488. https://doi.org/10.1016/j.bios.2015.11.098

6 Barashkova, P. S., Molodkina, L. M., & Korovina, M. D. (2017). Both sided irradiated track membrane in local water supply. *Magazine of Civil Engineering, 71*(3), 68–75. https://doi.org/10.18720/MCE.71.8

7 Russakova, A. V., Altynbaeva, L. Sh., Barsbay, M., Zheltov, D. A., Zdorovets, M. V., & Mashentseva, A. A. (2021). Kinetic and isotherm study of As(III) removal from aqueous solution by PET track-etched membranes loaded with copper microtubes. *Membranes, 11*(2), 116. https://doi.org/10.3390/membranes11020116

8 Novo, P., Dell'Aica, M., Jender, M., Höving, S., Zahedi, R. P., & Janasek, D. (2017). Integration of polycarbonate membranes in microfluidic free-flow electrophoresis. *Analyst, 142*(22), 4228–4239. https://doi.org/10.1039/C7AN01514C

9 Friedman, L. I., Hardwick, R. A., Daniels, J. R., Stromberg, R. R., & Ciarkowski, A. A. (1983). Evaluation of Membranes for Plasmapheresis. *Artificial Organs, 7*(4), 435–442. https://doi.org/10.1111/j.1525-1594.1983.tb04223.x

10 Wright, C. W., Li, N., Shaffer, L., Fowler, S. C., Howell, K. L., Kumar, G., Nelson, E., Seddon, J. M., & George, M. (2023). Establishment of a 96-well transwell system using primary human gut organoids to capture multiple quantitative pathway readouts. *Scientific Reports, 13*, 16357. https://doi.org/10.1038/s41598-023-43656-z

11 Yamashita, T., Inui, T., Yokota, J., Kawakami, K., Morinaga, G., Takatani, M., Kishimoto, W., Tomita, J., & Mizuguchi, H. (2021). Monolayer platform using human biopsy-derived duodenal organoids for pharmaceutical research. *Molecular Therapy — Methods & Clinical Development, 22*, 263–278. https://doi.org/10.1016/j.omtm.2021.05.005

12 George, J. H., Nagel, D., Waller, S., Hill, E. J., Parri, H. R., Coleman, M. D., Cui, Z., & Ye, H. (2018). A closer look at neuron interaction with track-etched microporous membranes. *Scientific Reports, 8*, Article 15552. https://doi.org/10.1038/s41598-018-33710-6

13 Ippolitov, D., Arreza, L., Munir, M. N., & Hombach-Klonisch, S. (2022). Brain Microvascular Pericytes—More Than Bystanders in Breast Cancer Brain Metastasis. In *Cells, 11*(8), 1263. https://doi.org/10.3390/cells11081263

14 Kumar, R., Harris-Hooker, S., Kumar, R., & Sanford, G. (2011). Co-culture of retinal and endothelial cells results in the modulation of genes critical to retinal neovascularization. *Vascular Cell, 3*, 27. https://doi.org/10.1186/2045-824X-3-27

15 Lu, Y., Ma, J., & Lin, G. (2019). Development of a two-layer transwell co-culture model for the in vitro investigation of pyrrolizidine alkaloid-induced hepatic sinusoidal damage. *Food and Chemical Toxicology, 129*, 391–398. https://doi.org/10.1016/j.fct.2019.04.057

16 Nishi, M., Tateishi, K., Sundararaj, J. S., Ino, Y., Nakai, Y., Hatayama, Y., Yamaoka, Y., Mihana, Y., Miyakawa, K., Kimura, H., Kimura, Y., Yamamoto, T., & Ryo, A. (2023). Development of a contacting transwell co-culture system for the in vitro propagation of primary central nervous system lymphoma. *Frontiers in Cell and Developmental Biology*, 11. https://doi.org/10.3389/fcell.2023.1275519

17 Haynes, J., Palaniappan, B., Tsopmegha, E., & Sundaram, U. (2022). Regulation of nutrient and electrolyte absorption in human organoid-derived intestinal epithelial cell monolayers. *Translational Research, 248*, 22–35. https://doi.org/10.1016/j.trsl.2022.04.008

18 Dokladny, K., In, J. G., Kaper, J., & Kovbasnjuk, O. (2021). Human epithelial stem cell-derived colonoid monolayers as a model to study shiga toxin-producing Escherichia coli–host interactions. *Methods in Molecular Biology, 2291*, 285–296. https://doi.org/10.1007/978-1-0716-1339-9_13

19 Kozuka, K., He, Y., Koo-McCoy, S., Kumaraswamy, P., Nie, B., Shaw, K., Chan, P., Leadbetter, M., He, L., Lewis, J. G., Zhong, Z., Charmot, D., Balaa, M., King, A. J., Caldwell, J. S., & Siegel, M. (2017). Development and Characterization of a Human and Mouse Intestinal Epithelial Cell Monolayer Platform. *Stem cell reports, 9*(6), 1976–1990. https://doi.org/10.1016/j.stemcr.2017.10.013

20 Bhatt, A. P., Gunasekara, D. B., Speer, J., Reed, M. I., Peña, A. N., Midkiff, B. R., Magness, S. T., Bultman, S. J., Allbritton, N. L., & Redinbo, M. R. (2018). Nonsteroidal Anti-Inflammatory Drug-Induced Leaky Gut Modeled Using Polarized Monolayers of Primary Human Intestinal Epithelial Cells. *ACS infectious diseases, 4*(1), 46–52. https://doi.org/10.1021/acsinfecdis.7b00139

21 Lyck, R., Enzmann, G., Lécuyer, M. A., Abadier, M., Bradfield, P. F., Biechele, T., Wegner, A., Rüegg, S., Shimshek, D. R., Herich, L. C., Merz, P. A., Engelhardt, B., & Weksler, B. (2016). ALCAM (CD166) is involved in extravasation of monocytes rather than T cells across the blood–brain barrier. *Journal of Cerebral Blood Flow & Metabolism, 37*(8), 2894–2909. https://doi.org/10.1177/0271678x16678639

22 Wimmer, I., Tietz, S., Nishihara, H., Deutsch, U., Sallusto, F., Gosselet, F., Lyck, R., Muller, W.A., Lassmann, H., Engelhardt, B. (2019). PECAM-1 stabilizes blood-brain barrier integrity and favors paracellular T-cell diapedesis across the blood-brain barrier during neuroinflammation. *Front. Immunol., 10*, 711. https://doi.org/10.3389/fimmu.2019.00711

23 Wilhelm, I., & Krizbai, I. A. (2014). In vitro models of the blood–brain barrier for the study of drug delivery to the brain. *Molecular Pharmaceutics, 11*(7), 1949–1963. https://doi.org/10.1021/mp500046f

24 Wong, A. D., Ye, M., Levy, A. F., Rothstein, J. D., Bergles, D. E., & Searson, P. C. (2013). The blood–brain barrier: an engineering perspective. *Frontiers in Neuroengineering, 6*, 7. https://doi.org/10.3389/fneng.2013.00007

25 Li, H.-X., Sun, X.-Y., Yang, S.-M., Wang, Q., & Wang, Z.-Y. (2018). Peroxiredoxin 1 promoted tumor metastasis and angiogenesis in colorectal cancer. *Pathology Research and Practice, 214*(5), 655–660. https://doi.org/10.1016/j.prp.2018.03.026

26 Zhao, J., Ma, X., & Xu, H. (2022). miR-29b-3p inhibits 22Rv1 prostate cancer cell proliferation through the YWHAE/BCL-2 regulatory axis. *Oncology Letters, 24*(2), 289. https://doi.org/10.3892/ol.2022.13409

27 Wei, Y., Wang, Y., Zang, A., Shang, Y., Song, Z., Wang, Z., Wang, Y., & Yang, H. (2018). Inducible T-cell co-stimulators regulate the proliferation and invasion of human hepatocellular carcinoma HepG2 cells. *Biological research, 51*(1), 2. https://doi.org/10.1186/s40659-017-0150-7

28 Pang, J., Li, G., Qian, H., Wu, Y., & Chen, Y. (2022). Secretory type II cGMP-dependent protein kinase blocks activation of PDGFRβ via Ser254 in gastric cancer cells. *Cell biology international, 46*(5), 747–754. https://doi.org/10.1002/cbin.1176629

29 Jeon, J. H., Kim, D. K., Shin, Y., Kim, H. Y., Song, B., Lee, E. Y., & Kim, J. K. (2016). Migration and invasion of drug-resistant lung adenocarcinoma cells are dependent on mitochondrial activity. *Experimental & Molecular Medicine, 48*, e277. https://doi.org/10.1038/emm.2016.129

30 Wasielewska, J. M., Chaves, J. C. S., Johnston, R. L., Milton, L. A., Hernández, D., Chen, L., Song, J., Lee, W., Leinenga, G., Nisbet, R. M., Pébay, A., Götz, J., White, A. R., & Oikari, L. E. (2022). A sporadic Alzheimer's blood-brain barrier model for developing ultrasound-mediated delivery of Aducanumab and anti-Tau antibodies. *Theranostics, 12*(16), 6826–6847. https://doi.org/10.7150/thno.72685

31 Varshavskaya, K. B., Petrushanko, I. Y., Mitkevich, V. A., Barykin, E.P., Makarov, A. A. (2024). Post-translational modifications of beta-amyloid alter its transport in the blood–brain barrier in vitro model. *Frontiers in Molecular Neuroscience, 17*, 1362581. https://doi.org/10.3389/fnmol.2024.1362581

32 Guo, B. B., Bellingham, S. A., & Hill, A. F. (2016). Stimulating the release of exosomes increases the intercellular transfer of prions. *Journal of Biological Chemistry, 291*(10). https://doi.org/10.1074/jbc.M115.684258

33 Rodrigues, P.V., de Godoy, J.V.P., Bosque, B.P., Carvalho, H.F. & Castro-Fonseca, M. (2022). Transcellular propagation of fibrillar α-synuclein from enteroendocrine to neuronal cells requires cell-to-cell contact and is Rab35-dependent. *Scientific Reports, 12*, 4168. https://doi.org/10.1038/s41598-022-08076-5

34 Hartmann, E. S., Schluessel, S., Köhler, M. I., Beck, F., Redeker, J. I., Summer, B., Schönitzer, V., Fottner, A., & Mayer-Wagner, S. (2020). Fibroblast-like cells change gene expression of bone remodelling markers in transwell cultures. *European Journal of Medical Research, 25*(1), 52. https://doi.org/10.1186/s40001-020-00453-y

35 Juste-Lanas, Y., Díaz-Valdivia, N., Llorente, A., Ikemori, R. & Alcaraz, J. (2023). 3D collagen migration patterns reveal a SMAD3-dependent and TGF-β1-independent mechanism of recruitment for tumour-associated fibroblasts in lung adenocarcinoma. *British Journal of Cancer, 128*(6), 967–981. https://doi.org/10.1038/s41416-022-02093-x

36 Bhatia, S. N., & Ingber, D. E. (2014). Microfluidic organs-on-chips. *Nature Biotechnology, 32*(8), 760–772. https://doi.org/10.1038/nbt.2989

37 Shimasaki, T., Yamamoto, S., Omura, R., & Takahiro Ochiya, T. (2021). Novel platform for regulation of extracellular vesicles and metabolites secretion from cells using a multi-linkable horizontal co-culture plate. *Micromachines, 12*(11), 1431. https://doi.org/10.3390/mi12111431

38 Henry, O. Y. F., Villenave, R., Cronce, M. J., Leineweber, W. D., Benz, M. A., & Ingber, D. E. (2017). Organs-on-chips with integrated electrodes for trans-epithelial electrical resistance (TEER) measurements of human epithelial barrier function. *Lab on a Chip, 17*(13), 2264–2271. https://doi.org/10.1039/c7lc00155j

39 Srinivasan, B., Kolli, A. R., Esch, M. B., Abaci, H. E., Shuler, M. L., & Hickman, J. J. (2015). TEER measurement techniques for in vitro barrier model systems. *Journal of laboratory automation, 20*(2), 107–126. https://doi.org/10.1177/2211068214561025

40 Ahmed Al-Tameemi, Z. K., Khanam, R., & Shetty, P. (2024). Bisphenol-A Leaching from Polycarbonate 5-Gallon Water Bottles in the UAE: A Comprehensive Study. *Nepal Journal of Epidemiology, 14*(1), 1301–1309. https://doi.org/10.3126/nje.v14i1.59934

41 Le, H. H., Carlson, E. M., Chua, J. P., & Belcher, S. M. (2008). Bisphenol A is released from polycarbonate drinking bottles and mimics the neurotoxic actions of estrogen in developing cerebellar neurons. *Toxicology letters, 176*(2), 149–156. https://doi.org/10.1016/j.toxlet.2007.11.001

42 Hoekstra, E. J., & Simoneau, C. (2013). Release of bisphenol A from polycarbonate: a review. *Critical reviews in food science and nutrition, 53*(4), 386–402. https://doi.org/10.1080/10408398.2010.536919

43 Wang, T., Han, J., Duan, X., Xiong, B., Cui, X. S., Kim, N. H., Liu, H. L., & Sun, S. C. (2016). The toxic effects and possible mechanisms of Bisphenol A on oocyte maturation of porcine in vitro. *Oncotarget, 7*(22), 32554–32565. https://doi.org/10.18632/oncotarget.8689

44 Cimmino, I., Fiory, F., Perruolo, G., Miele, C., Beguinot, F., Formisano, P., & Oriente, F. (2020). Potential Mechanisms of Bisphenol A (BPA) Contributing to Human Disease. *International journal of molecular sciences, 21*(16), 5761. https://doi.org/10.3390/ijms21165761

45 Li, T., Bian, B., Ji, R., Zhu, X., Wo, X., Song, Q., Li, Z., Wang, F., & Jia, Y. (2024). Polyethylene Terephthalate Microplastic Exposure Induced Reproductive Toxicity Through Oxidative Stress and p38 Signaling Pathway Activation in Male Mice. *Toxics, 12*(11), 779. https://doi.org/10.3390/toxics12110779

46 Zhang, H., Zhang, S., Duan, Z., & Wang, L. (2022). Pulmonary toxicology assessment of polyethylene terephthalate nanoplastic particles in vitro. *Environment international, 162*, 107177. https://doi.org/10.1016/j.envint.2022.107177

47 Apel, P., Bondarenko, M., Yamauchi, Y., & Yaroshchuk, A. (2021). Osmotic Pressure and Diffusion of Ions in Charged Nanopores. *Langmuir, 37*(48), 14089–14095. https://doi.org/10.1021/acs.langmuir.1c02267

48 International Organization for Standardization. (2011). ISO 10993-5:2011 IDT, medical devices. Evaluation of the biological effect of medical devices, Part 5, Cytotoxicity studies: in vitro methods.

49 Apel, P. Y., Velizarov, S., Volkov, A. V., Eliseeva, T. V., Nikonenko, V. V., Parshina, A. V., & Yaroslavtsev, A. B. (2022). Fouling and Membrane Degradation in Electromembrane and Baromembrane Processes. *Membranes and Membrane Technologies, 4*(2), 69–92. https://doi.org/10.1134/S2517751622020032

50 Sabbatovskii, K. G., Vilenskii, A. I., Sobolev, V. D., Kochnev, Y. K., & Mchedlishvili, B. V. (2012). Electrosurface and structural properties of poly(ethylene terephthalate) track membranes. *Colloid Journal, 74*(3), 328–333. https://doi.org/10.1134/S1061933X12010139

51 Apel, P. Y. (2013). *Track-etching. Encyclopedia of membrane science and technology*. Wiley. https://doi.org/10.1002/9781118522318.emst040

52 Lettmann, C., Mo Èckel, D., & Staude, E. (1999). Permeation and tangential flow streaming potential measurements for electrokinetic characterization of track-etched microfiltration membranes. *Journal of Membrane Science, 159*, 243–251. https://doi.org/10.1016/S0376-7388(99)00067-8

53 Déjardin, P., Vasina, E. N., Berezkin, V. V., Sobolev, V. D., & Volkov, V. I. (2005). Streaming potential in cylindrical pores of poly(ethylene terephthalate) track-etched membranes: Variation of apparent ζ potential with pore radius. *Langmuir, 21*(10), 4680–4685. https://doi.org/10.1021/la046913e

54 Chang, H. Y., Huang, C. C., Lin, K. Y., Kao, W. L., Liao, H. Y., You, Y. W., Lin, J. H., Kuo, Y. T., Kuo, D. Y., & Shyue, J. J. (2014). Effect of surface potential on NIH3T3 cell adhesion and proliferation. *Journal of Physical Chemistry C, 118*(26), 14464–14470. https://doi.org/10.1021/jp504662c

55 Chang, H. Y., Kao, W. L., You, Y. W., Chu, Y. H., Chu, K. J., Chen, P. J., Wu, C. Y., Lee, Y. H., & Shyue, J. J. (2016). Effect of surface potential on epithelial cell adhesion, proliferation and morphology. *Colloids and Surfaces B: Biointerfaces, 141*, 179–186. https://doi.org/10.1016/j.colsurfb.2016.01.049

56 Tamada, Y., Ikada, Y. (1993). Cell adhesion to plasma-treated polymer surfaces. *Polymer, 34*(10), 2208–2212.

57 Qiu, L., Hughes-Brittain, N., Bastiaansen, C., Peijs, T., & Wang, W. (2016). Responses of Vascular Endothelial Cells to Photoembossed Topographies on Poly(Methyl Methacrylate) Films. *Journal of Functional Biomaterials, 7*(4), 33. https://doi.org/10.3390/jfb7040033

58 Margel, S., Vogler, E. A., Firment, L., Watt, T., Haynie, S., & Sogah, D. Y. (1993). Peptide, protein, and cellular interactions with self-assembled monolayer model surfaces. *Journal of Biomedical Materials Research, 27*(12), 1463–1476. Portico. https://doi.org/10.1002/jbm.820271202

59 Rahmati, M., Silva, E. A., Reseland, J. E., A. Heyward, C., & Haugen, H. J. (2020). Biological responses to physicochemical properties of biomaterial surface. *Chemical Society Reviews, 49*(15), 5178–5224. https://doi.org/10.1039/d0cs00103a

60 Yi, B., Shen, Y., Tang, H., Wang, X., & Zhang, Y. (2020). Stiffness of the aligned fibers affects structural and functional integrity of the oriented endothelial cells. *Acta biomaterialia, 108*, 237–249. https://doi.org/10.1016/j.actbio.2020.03.022

61 Yi, B., Shen, Y., Tang, H., Wang, X., Li, B., & Zhang, Y. (2019). Stiffness of Aligned Fibers Regulates the Phenotypic Expression of Vascular Smooth Muscle Cells. ACS applied materials & interfaces, 11(7), 6867–6880. https://doi.org/10.1021/acsami.9b00293

62 Ghosh, S., Laha, M., Mondal, S., Sengupta, S., & Kaplan, D. L. (2009). In vitro model of mesenchymal condensation during chondrogenic development. Biomaterials, 30(33), 6530–6540. https://doi.org/10.1016/j.biomaterials.2009.08.019